

Laser-Induced Fluorescence and Bonding of Metal Dimers

V. E. Bondybey

Small metal clusters and related molecules have been the focus of increasing attention in recent years. This interest stems, in part, from the broader interest in catalysis and from the desire to understand, on a molecular level, the catalytic process. Metal surfaces are efficient catalysts for numerous industrially impor-

tant reactions. It is becoming clear that the catalytic activity is a function of not only the bulk metal composition but also the quality and preparation of the surface. Perfectly smooth surfaces are often relatively inactive as catalysts (1-3). Catalytic activity is improved by the presence of bumps and kinks on the surface and, in general, increases with the degree of material dispersion (4-6). Small metal particles exhibit increased catalytic efficiency beyond what would be expected based on the increased surface area. Extremely small, photolytically produced silver particles are catalysts in the classical photographic development process; clusters with approximately four silver atoms are the smallest entity effective in the catalysis (7).

Summary. This article describes a technique for the spectroscopic study of metal clusters and intermetallic compounds. First, metallic samples are vaporized by a pulsed YAG (yttrium-aluminum garnet) laser, and then the gaseous products are excited with a pulsed-dye laser until they fluoresce. A time-resolved, fluorescence spectrum is then measured by the product. The application of this technique to the study of metal dimers is reviewed, with emphasis on recent results from Be_2 and Cr_2 . Studies of such species often yield insights into the chemistry of metals and metal-metal bonding.

tant reactions. It is becoming clear that the catalytic activity is a function of not only the bulk metal composition but also the quality and preparation of the surface. Perfectly smooth surfaces are often relatively inactive as catalysts (1-3). Catalytic activity is improved by the presence of bumps and kinks on the surface and, in general, increases with the degree of material dispersion (4-6). Small metal particles exhibit increased catalytic efficiency beyond what would be expected based on the increased surface area. Extremely small, photolytically produced silver particles are catalysts in the classical photographic development process; clusters with approximately four silver atoms are the smallest entity effective in the catalysis (7).

Quite clearly, catalytic activity is strongly dependent upon the local micro-

scopic geometry and electronic structure of the metal particles. In order to understand in detail the catalytic action of the metal particles, and to answer questions such as why Ag_4 is an efficient catalyst while Ag_3 is not, a good understanding of the metal particles' fundamental properties is needed. Information about the geometry, electronic and vibrational structure, and dissociation energies of small metal particles is also necessary. Of particular interest are the questions of how such properties depend upon the number of atoms in the cluster and how quickly they converge to the collective properties of the bulk solid. Much of this information is obtainable from spectroscopic studies. Metal clusters have become a common ground to the otherwise diverse fields of spectroscopy, surface science, and catalysis.

Studies of small metal clusters are not new to spectroscopy. The first spectrum of a metal diatomic, Na_2 , was observed before the turn of the century (8). Only some 20 years later was the dimer correctly identified (9), but by the end of the 1930's the spectrum of Na_2 was analyzed and understood in fair detail, as were the

spectra of most of the other alkali dimers. In view of this interest in metal dimers in the early days of spectroscopy, it may come as a surprise how incomplete the present knowledge about them is. For scarcely one half of homonuclear metal diatomics are the ground electronic states well characterized (10), and only a few larger species have been studied spectroscopically. Substances usually denoted as metals encompass more than 75 percent of the periodic table, and they include elements with widely varied chemical and physical properties. They range from metals that are liquid at ambient temperatures, such as mercury or gallium, to elements that remain solid well above 3000°C . While some, such as the alkali, have properties making them well suited for spectroscopic studies—low melting points, high vapor pressures, and relatively strongly bound dimers—for many others the situation is much less favorable, and studies of them using classical spectroscopic techniques were not successful in detecting spectra of dimers or higher clusters.

In the case of nonmetallic elements, in particular carbon, quantum mechanical calculations now have considerable predictive power (11, 12). To a large extent, this is due to the availability of extensive experimental data—well-established geometries, lengths, and energies for various types of bonds, the basic building blocks of organic compounds. By comparison of calculations with good experimental data, the theoretical techniques have been continuously honed and refined. Although the intrinsic speed and capabilities of present-day computers, coupled with recent advances in theoretical techniques, should permit calculations of similar quality at least for the simpler and lighter metal clusters, the development of this field is hampered by the lack of sufficiently extensive experimental data.

More complete and reliable experimental information about small metal clusters—their spectroscopy, geometry,

The author is a member of the technical staff at AT&T Bell Laboratories in Murray Hill, New Jersey 07974.

and bonding—is sorely needed. Much progress has recently occurred in this field, mainly due to new spectroscopic techniques (13–22). The work in our laboratory includes both gas-phase and low-temperature matrix studies of small metal clusters, mainly by time-resolved, laser-induced fluorescence. In particular, a technique combining pulsed metal vaporization and detection of the products by fluorescence (23, 24) was quite successful in providing information, which is the main subject of this paper. We will first briefly discuss the experimental technique and its advantages and then cite a few of our recent results. In particular we will focus upon Be_2 and Cr_2 species that, in the past, were especially elusive in terms of both experimental characterization and theoretical understanding of their bonding.

Laser Vaporization of Metals

Spectroscopic characterization of metal clusters is often a nontrivial task. The experimental problem can be thought of in terms of two separate steps. In the first step, the metal vapor with adequate concentration of the species of interest has to be generated. In the second, the molecules have to be detected and characterized using a suitable spectroscopic technique. In traditional spectroscopic studies, the metal vapors were usually generated by heating the metal in furnaces and ovens while the detection was accomplished by optical absorption or, less frequently, emission spectroscopy.

A significant advance was made when laser-induced fluorescence was introduced into the second, detection step. The highly monochromatic laser beam excites only the molecules in direct resonance with the laser wavelength, which significantly reduces the complexity of the spectrum and facilitates its interpretation. Early studies used fixed frequency lasers for excitation and relied on accidental coincidences between the laser wavelength and the molecular transitions. For example, the elegant and detailed studies by Zare and co-workers have employed argon ion lasers for excitation of alkali dimers (25, 26).

Particularly convenient for laser-induced fluorescence are pulsed dye lasers. They are easy to operate and have a wide range of wavelengths that permits selective excitation of any particular quantum state. The use of pulsed excitation and detection also offers an opportunity for improvement of the first step, metal vapor production. While absorption studies or laser-excited fluorescence

studies with constant-wavelength lasers need a high steady-state concentration of the metal species, a study based on pulsed lasers requires the sample to be present only during the short, 10-nsec excitation pulse.

An experimental arrangement taking advantage of this fact, which we use in our studies, is shown in Fig. 1. The sample, S, in the form of a short, quarter-inch-diameter cylinder, is mounted inside a hole drilled through a copper block, B. The block itself is in thermal contact with the bottom of a Dewar flask of liquid nitrogen. The sample is vaporized by impinging a YAG (yttrium-aluminum garnet) laser pulse (27, 28) upon it through a quartz window, W. The hot plasma is immediately diluted with an excess of cold helium gas; and the supercooled, dense vapor is expanded through a 1-mm orifice into the probe region. There the gas is excited by the pulsed dye laser, which enters and exits the dye chamber through baffled sidearms. The pulsed dye laser (which typically produces ~ 0.1 to 0.5 mJ per 10-nsec pulse, 0.5-cm^{-1} spectral width) is suitably delayed following the vaporization pulse to allow for the time of travel needed by the sampled molecules to

reach the probed region. If necessary, the frequency of the laser beam is increased into the ultraviolet range (frequency doubled) by projecting the beam through angle-tuned KH_2PO_4 and $\text{KB}_5\text{O}_8 \cdot 4\text{H}_2\text{O}$ crystals. The fluorescence excited by the laser is collected with a lens and focused upon a photomultiplier, either directly or through a 0.5-m monochromator. The signal is amplified, digitized in a fast, 10 nsec per channel waveform recorder, averaged, and then further processed by a minicomputer that controls the experiment.

The amount of sample that is vaporized is very small; typically, less than $100\ \mu\text{g}$ of the metal are consumed per hour. This, however, corresponds to $>10^{13}$ atoms per pulse. The relative intensities of the atomic and molecular emissions suggest that, in favorable cases, up to 10 percent of the atoms are clustered and that there may be $>10^{12}$ dimer molecules. The number of molecules available in any given vibronic transition will be, at ~ 80 K, some two orders of magnitude lower. Such semi-quantitative considerations show that, in a particular quantum state, 10^5 to 10^8 molecules may be available.

The fact that such a small amount of material is consumed makes it feasible to perform, at reasonable cost, experiments with isotopically enriched samples. This is particularly useful in the case of some heavy metals with a large number of naturally occurring isotopes. For Sn_2 , in furnace experiments, the overlap of the spectra of the more than 50 isotopic molecular species results in a virtually continuous absorption. With laser vaporization, pure isotopic samples of Sn and Pb were studied, and the molecular constants of the dimers were determined (24, 29, 30).

Another area where laser vaporization is particularly useful is in the study of heteronuclear clusters. Very little is known about these species, and only a handful of the more than 2000 possible heteronuclear dimers are known (10). These molecules are readily prepared and studied by laser vaporization. One can prepare vapor of any desired composition by vaporizing either an alloy or, for immiscible metals, a pellet pressed from an appropriate mixture of metal powders. The SnBi molecule (31), which is isovalent with the CN radical, and the CuGa and CuIn molecules (32) are among the species that have been studied. While most studies of heteronuclear dimers were the by-product of work on homonuclear compounds, the technique is ideally suited for systematic studies of heteronuclear clusters.

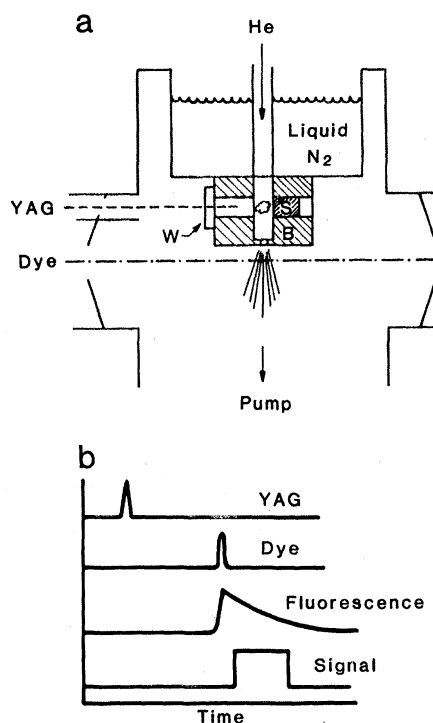


Fig. 1. (a) Schematic drawing of the experimental setup. The YAG (yttrium-aluminum garnet) laser impinges on the metal sample, S, and the vapors are swept by cold helium through a 1-mm orifice and are excited by the dye laser. The detector would be located behind the plane of the drawing. (b) The relative timing of the vaporization pulse, the dye-laser pulse, the laser-induced fluorescence, and the detector's electronic signal.

Metal-Metal Bonding: Spectra and Properties of Be₂

The simplest possible metal dimer, Li₂, and its properties are known experimentally (10) and understood theoretically. However, for the next heavier dimer species, Be₂, things are quite different. Gas-phase studies have consistently failed to provide spectra attributable to Be₂. On the other hand, Be clusters have become a favorite test case for theoreticians, and Be₂ has been studied rather extensively computationally (33–39).

Predictions from the simplest molecular-orbital theory are shown in Fig. 2. Bonding in both Li₂ and Be₂ is governed by the 2s valence electrons. Combination of the two atomic 2s orbitals will give rise to one bonding, σ_g , and one antibonding, σ_u , molecular orbital. The two available 2s electrons in the Li₂ ground state would just fill the lowest energy, bonding σ_g orbital, resulting in a relatively strong single bond. Since Be has, however, two 2s electrons, both the σ_g and σ_u^* orbitals will be occupied by two electrons in the Be₂ ground state. On the simplest level of theory, ground state Be₂ is thus predicted to be unbound. Thus, studies of Be₂, which include a wide range of theoretical techniques and varying levels of sophistication, show little agreement. They range from Hartree-Fock calculations (33–35), which yield a completely repulsive ground state, to density-functional calculations (37), which predict a bond of ~ 3000 cm⁻¹ binding energy. Configuration-interaction (CI) calculations (35), which include single and double excitations, predict a bond of ~ 45 cm⁻¹ with $r_e = 4.6$ Å, whereas two more recent CI calculations (38, 39) seem to agree upon a somewhat stronger potential with ~ 700 cm⁻¹ binding energy and an r_e of ~ 2.45 Å. Overall, more than 30 theoretical studies have appeared in the last 5 to 6 years dealing with the Be₂ bond potential, a lot of attention for a molecule whose existence was in doubt.

Beryllium has a much higher boiling point and lower vapor pressure than the alkali; this makes it difficult to study experimentally. Furthermore, in view of the predicted low binding energy, it may be difficult to find equilibrium conditions under which Be₂ has an appreciable concentration in the metal vapor. In circumstances like these, the laser vaporization technique, which produces dense, supersaturated vapors, is particularly valuable (40). By controlling conditions and sampling the dense vapors at various stages of the clustering process, species can be

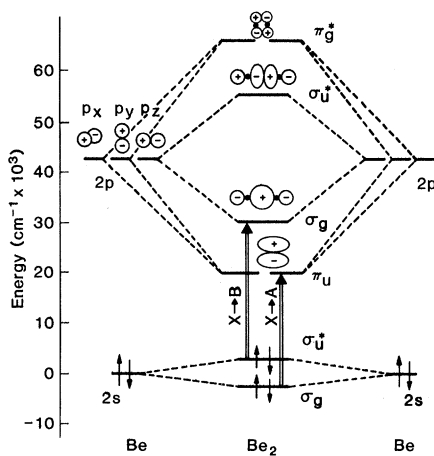


Fig. 2. Molecular orbitals of Be₂. The double arrows denote the two allowed electronic transitions discussed in this article.

studied that are quite scarce under equilibrium conditions.

Since in our experiment the molecules are detected by means of electronic fluorescence, the properties and bonding of excited electronic states of Be₂ should be considered. As noted above, two ground state, $2s^2$ ¹S, Be atoms give rise to only one electronic state, the ground state, which is labeled X¹ Σ_g^+ . Neglecting the $2s^2$ ¹S + $2s2p$ ³P limit, which gives rise only to triplet states, the lowest excited singlet states will correspond to $2s^2$ ¹S + $2s2p$ ¹P, that is, with one Be atom in the ¹P state at 42,565.3 cm⁻¹. Referring again to Fig. 2, the triply degenerate 2p orbitals will also split as the molecule is formed, creating two bonding (π_u and σ_g) and two antibonding (σ_u and π_g) molecular orbitals. These will give rise to two orbitally allowed electronic transitions, as shown in the diagram by arrows. One of these transitions will promote an antibonding 2s σ_u electron, into the bonding 2p σ_g orbital, giving rise to an electronic state labeled ¹ Σ_u^+ . An absorption observed by Weltner and co-workers (41) in solid matrices was attributed to this transition. The other transition will promote one of the bonding, 2s σ_g electrons into the 2p π_u orbital, resulting in a state labeled ¹ Π_u . Since this ¹ Π_u state will have two bonding and two antibonding electrons, it might be predicted to be only weakly bound, like the ground electron state, or repulsive. Actually, statistical arguments based on counting bonding electrons fail here, demonstrating the limitations of oversimplified molecular orbital theory. The π_u orbital has a much stronger bonding character than the σ_g orbitals, and the data presented below indicate that the ¹ Π_u state is, in fact, very strongly bound.

At room temperature the beryllium

vapor produced by laser vaporization reveals strong signals from Be atomic transitions and weaker signals from Be⁺ cations. In addition, bands from BeO and BeH are observed, as well as several spectra clearly from polyatomic species. However, when the temperature of the gas flow is lowered to ~ 77 K by liquid nitrogen, two additional, strong band systems appear with origins at 27,857.8 cm⁻¹ and 21,678.4 cm⁻¹ (40). The higher energy transition, whose 0'–0" band is reproduced in Fig. 3a, is characterized by a progression in a vibrational frequency of ~ 510 cm⁻¹, and a very short lifetime, < 20 nsec. Rotational analysis reveals a simple structure, with only P and R branches present, showing that the electronic angular momentum $\Lambda = 0$ in both electronic states. This is consistent with this band's assignment to an electron transition in diatomic Be₂ labeled B¹ Σ_u^+ \leftrightarrow X¹ Σ_g^+ . The lower energy progression, exhibiting a vibrational frequency (ω_e) of 686 cm⁻¹, is then due to the transition labeled A¹ Π_u \leftrightarrow X¹ Σ_g^+ . As shown in Fig. 3b, these bands exhibit a prominent Q branch, characteristic of a transition with $\Delta\Lambda = 1$. This spectrum is somewhat less intense than the ultraviolet B¹ Σ_u^+ spectrum, and the A¹ Π_u emission exhibits a longer lifetime, ~ 190 nsec. The rotational lines of both transitions exhibit an intensity alternation with a ratio of 5:3, characteristic for Be₂ (with nuclear spin of 3/2). Also, consistent with the ¹ Σ_g^+ ground state, spectral lines corresponding to odd values of the rotational quantum number, J , appear with greater intensity than other spectral lines.

Both electronic transitions show the presence of several weak "hot" bands due to residual population of the excited vibrational state, $v'' = 1$, which yields a value of $\Delta G_{1/2} = 223.4$ cm⁻¹. The population of higher vibrational states is apparently low, and no bands with $v'' > 1$ were detected in the excitation spectra. More information about the ground state potential could be obtained by studies of the dispersed fluorescence. The emission spectra consist of several sharp bands at the blue end of the spectrum followed by several broad maxima extending through the visible region. The discrete structure in the spectra corresponds to emission that results in the bound molecule occupying one of its lower vibrational levels. While the first two emission bands are spaced by $\sim 223 \pm 3$ cm⁻¹, consistent with the $\Delta G_{1/2} = 223.4$ cm⁻¹ deduced from the excitation spectrum, the next intervals are only $\sim 170, 122, \text{ and } 79 \pm 3$ cm⁻¹. Bands with $v'' > 5$ could not be resolved. This fast

convergence is consistent with the theoretical predictions of low bonding energy and explains the observed disappearance of the Be_2 signal when the gas flow temperature is allowed to rise from 77 K to 300 K. It is caused by thermal dissociation; the equilibrium constant for the reaction $\text{Be}_2 \rightarrow 2\text{Be}$ changes by many orders of magnitude over this range with the equilibrium at room temperature being completely on the side of dissociated atoms (42).

Broad intensity fluctuations in the emission spectra, with areas of zero intensity in between represent the "internal diffraction" predicted by Condon some 40 years ago for "bound-free" transitions that result in separated atoms (43, 44). The intensity variations result from the phase relationship between the wave functions for the initial and final

states with the minima corresponding to the nodes of the wave function of the emitting vibrational level. The intensity distribution thus contains information about the ground state potential. Analysis of such spectra, as well as studies of the discrete region at higher resolution could provide detailed information about the electronic ground state.

Spectroscopic information obtained from the analysis of Be_2 spectra is compiled in Table 1 and compared with similar data for Li_2 . Both the excited states of Be_2 are rather strongly bound, with rather high vibrational frequencies and short internuclear distances. Even more interesting is the ground electronic state and its molecular constants which exhibit unusual characteristics. Based on the short r_e , internuclear distance, and relatively high vibrational frequency, ω_e ,

Be_2 appears to be similar to Li_2 , that is, reasonably strongly bound. On the other hand, the dissociation energy, $D_0 \sim 800 \text{ cm}^{-1}$, as deduced from the emission spectrum is indicative of a rather weak bond. The $2s$ valence electrons of beryllium, which have to provide the molecular bonding, are subject to a larger effective nuclear charge than the $2s$ electrons of lithium, and this results in a more compact electronic wave function. The optimum overlap will therefore occur at a shorter internuclear distance. The overall bonding results from a fine balance between the attractive contributions and the repulsive terms from the antibonding electrons. The result is the relatively weak bond; however, if the molecule is to be bound at all, the bond has to be relatively short, assuring effective overlapping of the $2s$ wave functions.

Two particularly interesting issues are in what way and how quickly the properties of discrete molecules change and approach the collective properties of the bulk metal as the cluster size is increased. Virtually nothing is known about the structures and properties of intermediate size clusters, but it is instructive to compare the diatomic Li_2 and Be_2 with the respective metals. Some of the relevant properties are compared in Table 1. The dissociation energy of Li_2 is $\sim 8450 \text{ cm}^{-1}$. On the other hand, it takes $13,500 \text{ cm}^{-1}$ to remove an Li atom from bulk metal, so the energy per bond (with eight nearest neighbors in the solid and counting half a bond per neighbor) is 3400 cm^{-1} . The diatomic is thus more strongly bound, and this is reflected in a shorter bond distance ($r_e = 2.673 \text{ \AA}$) as opposed to the 3.039-\AA metal-metal distance in the solid.

The situation in beryllium is quite different. While the diatomic dissociation energy, D_0 , is $\sim 800 \text{ cm}^{-1}$, the energy per bond in the metal (12 nearest neighbors) is $\sim 4500 \text{ cm}^{-1}$, and $\sim 27,100 \text{ cm}^{-1}$ are required to remove a Be atom from the bulk metal. Similarly, the diatomic Be_2 has an $r_e = 2.46 \text{ \AA}$, considerably longer than the metal-metal distance in the solid, 2.226 \AA .

These small metal clusters behave quite differently than the corresponding solids. Obviously, it would be very difficult to predict metal structure and properties based on the known properties of the diatomic alone. Conversely, one can not, at present, reliably deduce the properties of small clusters based on the knowledge of the solid.

As the size of the cluster is increased, the properties have to approach those of the solid. Thus, the dissociation energy

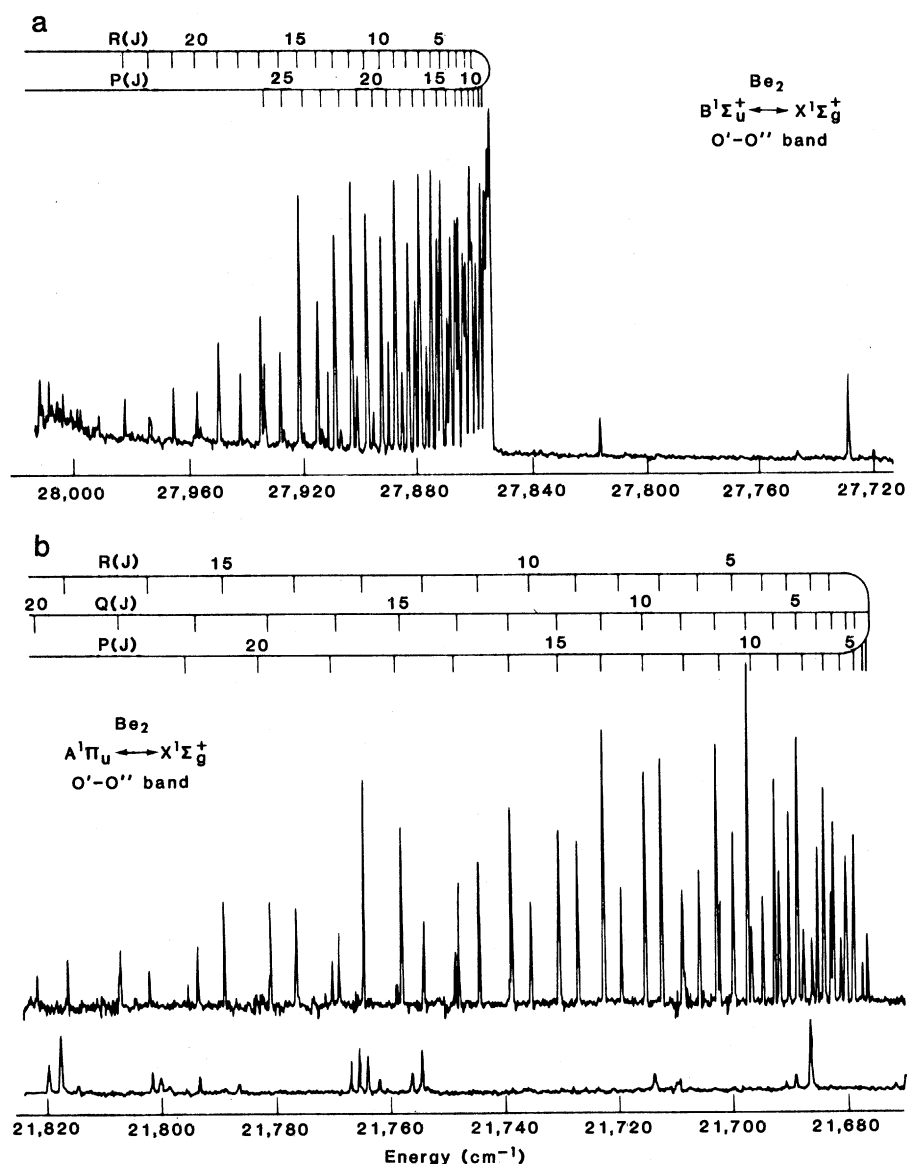


Fig. 3. Sections of the low-resolution spectra of Be_2 , showing the J numbering; (a) $0'-0''$ band of the $B^1\Sigma_u^+ \leftrightarrow X^1\Sigma_g^+$ transition; (b) $0'-0''$ band of the $A^1\Pi_u \leftrightarrow X^1\Sigma_g^+$ transition; note the presence of a Q branch. The lower trace in (b) shows a simultaneously recorded optogalvanic calibration spectrum of uranium.

of beryllium clusters has to converge at the $27,100 \text{ cm}^{-1}$ cohesive energy of the bulk metal, and the polyatomic species should be much more strongly bound than the diatomic. Since, as the present study shows, the diatomic molecules are efficiently formed in our experiments, one might expect that larger species should also be present. The excitation spectra of the laser vaporization products of beryllium do indeed exhibit several band systems clearly due to polyatomic species. Their assignment to specific molecular species will, however, require additional work.

Time-Resolved Fluorescence and Weak Electronic Transitions

A difficult spectroscopic problem arises when a relatively weak electronic transition of interest is overlapped by a much stronger spectrum of the same molecule. Such a situation occurs in S_2 and Se_2 , where the orbitally allowed $\text{X}^3\Sigma_g^+ \leftrightarrow \text{A}^3\Pi_u$ transition is overlapped by the much stronger $\text{X}^3\Sigma_g^+ \leftrightarrow \text{B}^3\Sigma_u^+$ (45). Numerous attempts to characterize the $\text{A}^3\Pi_u$ state in the gas phase met with little success. In pulsed laser studies one can take advantage of the time-resolved nature of the experiment (46). The weaker transition is typically characterized by a much longer fluorescence lifetime, so by selectively monitoring emissions that occur after a suitable delay, one can separate the weak transition from the overlapping stronger spectrum.

A result of such an experiment (47) is shown in Fig. 4, where the laser wavelength was scanned through the range of one dye. To obtain the top trace, the digitized signal from the first 100 nsec was integrated; it shows bands due to the strong $\text{X}^3\Sigma_g^+ \leftrightarrow \text{B}^3\Sigma_u^+$ transition. The bottom trace, where the signal in the 500 to 2000 nsec interval was integrated, shows a completely different spectrum which is easily assigned to the elusive $\text{X}^3\Sigma_g^+ \leftrightarrow \text{A}^3\Pi_u$ transition. This was fully confirmed by a detailed rotational analysis of a high resolution spectrum, which also gave the spectroscopic constants of the $\text{A}^3\Pi_u$ state.

d Electrons and Transition Metal

Bonding: Vibrational Frequency of Cr_2

The bonding and spectroscopy of main group elements are now reasonably well understood. From the theoretical point of view, the state of the art appears fairly satisfactory with, in most cases, reasonable agreement between quantum me-

chanical computations and experimental data. Quite different is the situation concerning transition metals. Until a few years ago, Cu_2 appeared to be the only diatomic molecule of this category whose gas phase spectra were well characterized.

The electronic structure and bonding of the main group elements is characterized by the s and p valence electrons with a completely filled inner core. In transition metals, on the other hand, the outermost shell is preceded by slightly deeper-lying, partially filled d orbitals. Chromium and the Cr_2 diatomic represent a particularly simple and interesting example of this class. The ground state

of Cr atoms, $3d^5 4s^1$, like a potassium atom, has a single $4s$ electron in its valence shell. In addition, it has a half-filled $3d$ level with five electrons. The importance of Cr_2 for understanding transition metal bonding has been noted by the theoreticians, and a large number of quantum mechanical calculations on this molecule have appeared (48-51). However, there is little agreement between the work.

Recent, extensive CI calculations by Goodgame and Goddard predict only a shallow Van der Waals minimum at $r_e = 4.5 \text{ \AA}$ (48). Other work, on the other hand, concludes that Cr_2 is a strongly bound molecule with short internuclear

Table 1. Molecular constants of Be_2 and Li_2 . The $\nu_{0,0}$ value is the difference in energy between the primary vibrational levels of the ground state and excited state; ω_e is the vibrational frequency in terms of wavenumbers; $\omega_e x_e$, the anharmonic vibrational frequency in terms of wavenumbers; r_e is the equilibrium internuclear distance; and D_0 is the dissociation energy. The spectroscopic constants for Li_2 are from (10).

Electronic state	$\nu_{0,0}$ (cm^{-1})	ω_e (cm^{-1})	$\omega_e x_e$ (cm^{-1})	r_e (\AA)	D_0 (cm^{-1})
$\text{Be}_2, \text{X}^1\Sigma_g^+$	0.0	223.4*	(26)	2.465	(800)
$\text{Be}_2, \text{A}^1\Pi_u$	21,678.4	685.7	4.85	1.983	21,500
$\text{Be}_2, \text{B}^1\Sigma_u^+$	27,857.8	504.0	5.0	2.16	15,300
Be metal				2.226†	27,100‡
$\text{Li}_2, \text{X}^1\Sigma_g^+$	0.0	351.43	2.61	2.673	8,437
$\text{Li}_2, \text{A}^1\Sigma_u^+$	14,020.6	255.47	1.58	3.107	9,300
$\text{Li}_2, \text{B}^1\Pi_u$	20,395.3	270.12	2.67	2.935	2,950
Li metal				3.039†	13,500‡

* $\Delta G_{1/2}$ value. †Nearest neighbor distance. ‡Atomization energy.

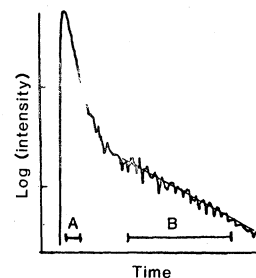
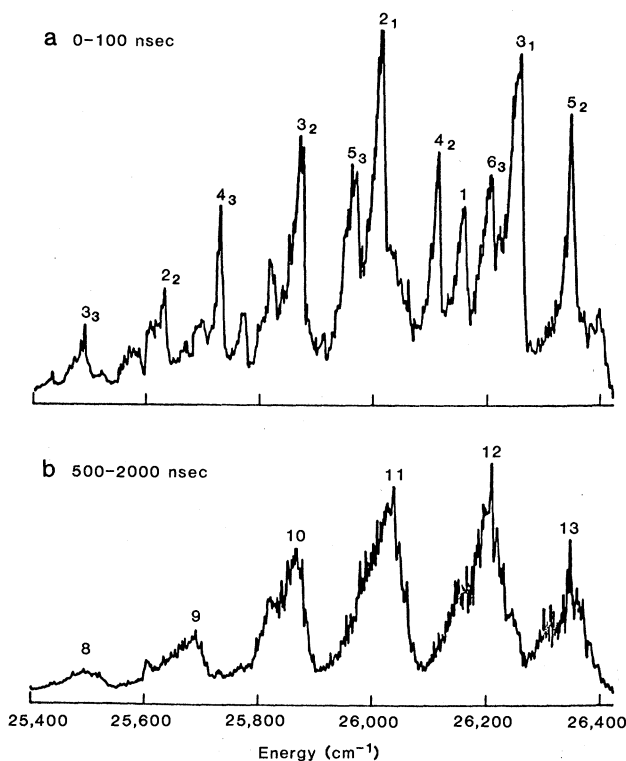


Fig. 4. Spectra of Se_2 obtained from a single scan through the range of the Pilot 386 dye. The inset (above) shows typical double-exponential fluorescence decay. (a) Spectrum obtained from the short-lived emission, within the limits denoted by A in the inset, is integrated; vibrational quantum numbers ν' , assigned to the $\text{B}^3\Sigma_u^- \leftrightarrow \text{X}^3\Sigma_g^-$ bands are shown, with all $\nu' \neq 0$ given as subscripts. (b) Integration between the limits denoted B in the inset shows the long lived A ($0_u^+ \leftrightarrow \text{X}^3\Sigma_g^- (0_g^+)$) emission. The ν' numbering is shown.

distance and, presumably, a high bond order (49). The individual studies do not even agree on the symmetry of the ground state, with $^1\Sigma_g^+$, $^3\Sigma_u^+$, $^1\Sigma_g^+$, $^1\Sigma_u^+$, and $^1\Pi$ being the possibilities suggested. The source of these problems and, presumably, of the difficulties of the quantum mechanical calculations, lies in the uncertainty about the role of the d electrons in transition metal bonding. If the bonding is provided by the $4s$ electrons alone, with the $3d$ electrons inactive and localized on the chromium nuclei, a high-multiplicity $^1\Sigma_u^+$ ground state, which is essentially isovalent with a ground state of potassium dimer, would result. The dimer would have a relatively weak single bond. On the other end of the scale, the $3d$ electrons could combine to form five bonding molecular orbitals, one of which would be a σ orbital, two π orbitals, and two δ orbitals. In this model, Cr_2 would be characterized by a very strong, sextuple bond, and it would have a $^1\Sigma_g^+$ ground state.

Experimental studies show that, although neither model fits perfectly, the molecule is much closer to the latter, strongly bonded model (52–55). Laser-induced fluorescence spectrum of Cr_2 produced by laser vaporization of chromium metal is shown in Fig. 5. The spectrum is very simple, as would be expected for a $^1\Sigma_g^+ \leftrightarrow \Sigma_u^+$ transition. In addition to the 0–0 band, a very weak 1–0 band was detected 452 cm^{-1} lower in energy. Molecular constants of Cr_2 derived from spectral analysis are listed in Table 2 and compared with the corresponding properties of K_2 and Cu_2 . Again, the individual pieces of information are somewhat contradictory. The $1.67\text{-}\text{\AA}$ internuclear distance, r_e , in the Cr_2 ground state represents the shortest known metal-metal bond and is shorter by some 30 percent than the Cr–Cr nearest-neighbor distance in chromium metal. Similarly, the 452 cm^{-1} vibrational frequency is unexpectedly high when compared with the 92 cm^{-1} frequency of

potassium dimer; it implies a force constant more than 30 times that of K_2 . These values are certainly consistent with an extremely strong, high-order bond. On the other hand, the experimentally determined Cr_2 dissociation energy, while higher than that of K_2 , is indicative of only a moderately strong bond.

The seeming contradictions arise from the fact that although all the 12 valence electrons of Cr_2 are paired in formally bonding molecular orbitals, they do not contribute equally to the molecular bond. In the absence of contributions from the $3d$ electrons, the $4s$ electrons would provide the bonding, and the chromium dimer would probably have a bond length similar to or somewhat shorter than the r_e value of 3.9051 \AA in K_2 . On the other hand, to accomplish effective overlapping of the $3d$ wavefunctions, a much shorter bond length is required. At the experimental r_e , 1.67 \AA , the $4s$ electrons contribute little to the bonding; possibly, they are even slightly antibonding. Furthermore, the $3d$ electrons do not contribute equally to the binding, with the δ bonds probably being rather weak. Thus, the bond length is determined by the d electrons while the overall bond energy results from a balance between the bonding contributions from the d electrons and the repulsive interactions of the other electrons.

Table 2. Molecular constants of Cr_2 the related diatomics compared to those of K_2 and Cu_2 . The parameters are defined in Table 1. The constants for Cr_2 are from (51, 54); the data for K_2 and Cu_2 are from (10).

Electronic state	$\nu_{0,0}$ (cm^{-1})	ω_e (cm^{-1})	$\omega_e x_e$ (cm^{-1})	r_e (\AA)	D_0 (cm^{-1})
Cr_2 , $X^1\Sigma_g^+$		452.34*		1.679	12,500
Cr_2 , $A^1\Sigma_u^+$	21,751.42	(415) *		1.690	14,100
Cr metal				2.498†	33,200‡
K_2 , $X^1\Sigma_g^+$		92.02	0.2829	3.905	4,150
K_2 , $A^1\Sigma_u^+$	11,681.9	69.09	0.153		
K metal				4.544†	7,490‡
Cu_2 , $X^1\Sigma_g^+$		264.55	1.025	2.2197	16,400
Cu_2 , $B^1\Sigma_u^+$	21,747.88	242.15	2.0	2.3726	
Cu metal				2.556†	28,200‡

* $\Delta G_{1/2}$ values. †Nearest neighbor distance. ‡Atomization energy.

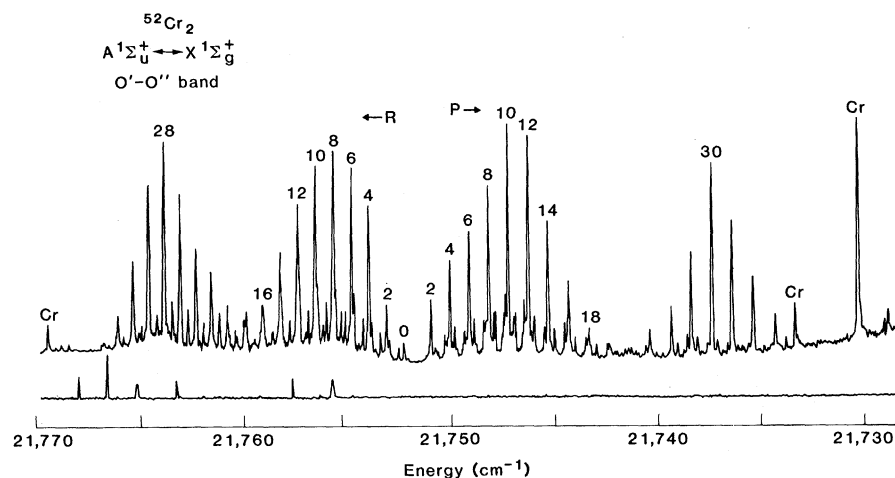


Fig. 5. High-resolution scan of the $0'-0''$ band from the $A^1\Sigma_u^+ \leftrightarrow X^1\Sigma_g^+$ transition of Cr_2 . Rotational numbering is shown for $^{52}\text{Cr}_2$; weaker lines appearing in the spectrum are due to $^{52}\text{Cr}-^{50}\text{Cr}$ and $^{54}\text{Cr}-^{52}\text{Cr}$. Several lines distinguished by longer lifetime and due to atomic chromium are labeled. The bottom trace shows a simultaneously recorded optical galvanic calibration spectrum of uranium.

Summary

Laser vaporization of metals and pulsed, laser-fluorescence spectroscopy of the dense, supersaturated vapors are shown to be useful techniques for metal cluster studies. Analysis of the spectra yields interesting insights into the metal-metal bonding. Thus Be_2 is found to have a relatively weakly bound ground state with, however, a surprisingly short bond length and a high value for the vibrational frequency. Diatomic chromium, Cr_2 , has an extremely short internuclear distance, $r_e = 1.68\text{ \AA}$, and a high vibrational frequency, $\omega_e = 452\text{ cm}^{-1}$, but only a moderately strong bond. While in this article I have focused attention on diatomic species, the technique is equally applicable to polyatomic clusters, as long as they possess bound excited states with an appreciable quantum yield of fluorescence.

References and Notes

- G. A. Somorjai, *Acc. Chem. Res.* **9**, 248 (1976).
- S. L. Bernasek and G. A. Somorjai, *J. Chem. Phys.* **62**, 3149 (1975).
- H. F. Schaefer, *Acc. Chem. Res.* **10**, 287 (1977).
- A. L. Robinson, *Science* **185**, 772 (1974).
- J. H. Sinfelt, *Acc. Chem. Res.* **10**, 15 (1977).
- , *Science* **195**, 641 (1977).

7. J. F. Hamilton and P. C. Logel, *Photogr. Sci. Eng.* **18**, 507 (1974).
8. H. E. Roscoe and A. Schuster, *J. Chem. Soc.* **27**, 942 (1874); E. Wiedemann and G. C. Schmidt, *Ann. Phys. (Leipzig)* **57**, 447 (1896).
9. H. G. Smith, *Proc. R. Soc. London, Ser. A* **106**, 400 (1924).
10. K. P. Huber and G. Herzberg, *Constants of Diatomic Molecules* (Van Nostrand, New York, 1981).
11. J. A. Pople, R. Seeger, K. Raghavachari, *Int. J. Quantum Chem. Symp.* **11**, 149 (1977).
12. H. F. Schaeffer, Ed., *Modern Theoretical Chemistry* (Plenum, New York, 1977).
13. K. Sattler, J. Muhlbach, E. Recknagel, *Phys. Rev. Lett.* **45**, 821 (1980).
14. A. Herrmann, E. Schumacher, L. Woste, *J. Chem. Phys.* **68**, 2327 (1978).
15. J. L. Gole, G. J. Green, S. A. Pace, D. R. Preuss, *ibid.* **76**, 2247 (1982).
16. T. G. Dietz, M. A. Duncan, D. E. Powers, R. E. Smalley, *ibid.* **74**, 6511 (1981).
17. V. E. Bondybey and J. H. English, *ibid.* **73**, 42 (1980).
18. G. A. Ozin, *Catal. Rev., Sci. Eng.* **16**, 191 (1977).
19. D. M. Lindsay and G. A. Thompson, *J. Chem. Phys.* **77**, 1114 (1982).
20. D. P. DiLella, W. Limm, R. H. Lipson, M. Moskovits, K. V. Taylor, *ibid.*, p. 5263.
21. J. C. Miller and L. Andrews, *Appl. Spectrosc. Rev.* **16**, 1 (1980).
22. C. A. Baumann, R. J. VanZee, S. V. Bhatt, W. Weltner, *J. Chem. Phys.* **78**, 190 (1983).
23. V. E. Bondybey and J. H. English, *ibid.* **74**, 6978 (1981).
24. ———, *ibid.* **76**, 2165 (1982).
25. W. Demtröder et al., *ibid.* **51**, 5495 (1969).
26. R. Velasco et al., *ibid.*, p. 5522.
27. P. Ohez, P. Jaegle, S. Leach, M. Velghe, *J. Appl. Phys.* **40**, 2545 (1969); R. A. Bingham and P. L. Salter, *Anal. Chem.* **48**, 1735 (1976).
28. K. A. Lincoln, *J. Mass. Spectrosc. Ion Phys.* **2**, 75 (1969).
29. V. E. Bondybey, M. Heaven, T. A. Miller, *J. Chem. Phys.* **78**, 3593 (1983).
30. M. Heaven, T. A. Miller, V. E. Bondybey, *ibid.* **87**, 2072 (1983).
31. V. E. Bondybey and J. H. English, *ibid.* **79**, 4746 (1983).
32. V. E. Bondybey, G. P. Schwartz, J. H. English, *ibid.* **78**, 11 (1983).
33. P. E. Cade and A. C. Wahl, *At. Data Nucl. Data Tables* **13**, 339 (1974).
34. C. F. Bender and E. R. Davidson, *J. Chem. Phys.* **47**, 4972 (1967).
35. C. E. Dykstra, H. F. Schaeffer, W. Meyer, *ibid.* **65**, 5141 (1976).
36. M. R. A. Blomberg and P. E. M. Siegbahn, *Int. J. Quantum Chem.* **14**, 583 (1978).
37. R. O. Jones, *J. Chem. Phys.* **71**, 1300 (1979).
38. R. J. Harrison and N. C. Handy, *Chem. Phys. Lett.* **98**, 97 (1983).
39. B. H. Lengsfeld, A. D. McLean, M. Yoshimine, B. Liu, *J. Chem. Phys.* **79**, 181 (1983).
40. V. E. Bondybey and J. H. English, *ibid.* **80**, 568 (1984); V. E. Bondybey, *Chem. Phys. Lett.* **109**, 436 (1984).
41. J. M. Brom, W. D. Hewett, W. Weltner, *ibid.* **62**, 3122 (1975).
42. D. J. Frurip calculated the thermodynamic properties and equilibrium constants of Be₂ from our experimental data.
43. E. U. Condon, *Phys. Rev.* **32**, 858 (1928).
44. D. L. Rousseau and P. F. Williams, *Phys. Rev. Lett.* **33**, 1368 (1974).
45. K. K. Yee and R. F. Barrow, *J. Chem. Soc., Faraday Trans. 2* **68**, 1181 (1972).
46. J. G. Pruett and R. N. Zare, *J. Chem. Phys.* **62**, 2050 (1975).
47. M. Heaven, T. A. Miller, J. H. English, V. E. Bondybey, *Chem. Phys. Lett.* **91**, 251 (1982).
48. M. M. Goodgame and W. A. Goddard, *Phys. Rev. Lett.* **48**, 135 (1982).
49. A. B. Anderson, *J. Chem. Phys.* **69**, 4046 (1976); W. Klotzbüchen and G. A. Ozin, *Inorg. Chem.* **16**, 984 (1977).
50. J. Harris and R. O. Jones, *ibid.* **70**, 830 (1979).
51. P. Correa de Mello, W. D. Edwards, M. C. Zerner, *J. Am. Chem. Soc.* **104**, 440 (1982).
52. Y. M. Efremov, A. N. Samoilova, L. V. Gurvich, *Opt. Spectrosc. (U.S.S.R.)* **36**, 381 (1974).
53. D. L. Michalopoulos, M. E. Geusic, S. G. Hansen, D. E. Powers, R. E. Smalley, *J. Phys. Chem.* **86**, 3914 (1982).
54. S. J. Riley, E. K. Parks, L. G. Pobo, S. Wexler, *ibid.* **79**, 2577 (1983).
55. V. E. Bondybey and J. H. English, *Chem. Phys. Lett.* **94**, 443 (1983).
56. I thank K. Raghavachari for our useful discussions and T. Dunning for providing theoretical potentials of Be₂⁺ prior to publication.

The 1984 Nobel Prize in Physics

The 1984 Nobel Prize in Physics was shared between Carlo Rubbia and Simon Van der Meer. Rubbia and Van der Meer were recognized for "their decisive contributions to the large project, which led to the discovery of the field particles W and Z, communicators of the weak interaction."

The massive experiment, carried out at CERN, the European Center for Nuclear Research, which is located near Geneva, involved two major innovations. One had to do with accelerator science, the other with particle detectors. The results were announced early in 1983, making this one of the shortest "waiting" intervals in Nobel history.

Simon Van der Meer is a soft-spoken and gifted inventor with a high order of analytical ability. He was born in 1925 and is a graduate of the Technische Hogeschool in Delft. His invention of "stochastic cooling" is subtle and required insight and the ability to do rather complex, statistical calculations. It was a crucial element in the process of discovering the W and Z particles.

Carlo Rubbia, 50, is an exuberant extrovert, famous in his circle for unlimited energy and enthusiasm combined with a

broad-ranging and deep understanding of physics. He attended the Scuola Normale in Pisa, where his teachers frequently compared him with a famous predecessor, Enrico Fermi. In the course of his Nobel research, Rubbia worked hard on the accelerator problems, assembled the group of over 100 Ph.D.'s, and led them in the design and construction of the most complex particle detector ever built. He found time to fulfill his obligations as professor of physics at Harvard, helping, in the course of his commuting between Cambridge and CERN, to alleviate the financial plight of several airlines.

The identification of the W and Z culminates a 50-year history of the weak force. The first suggestion that the weak interaction is mediated through an intermediate boson field was made by Yukawa (*I*) in his 1935 paper which proposed that the strong forces holding nuclei together were communicated by a massive particle, later named the pion. Yukawa hoped that the exchange of pions would also do for the weak force. However, after the fall of parity in 1957, the structure of the weak force required a spin 1 (vector) mediator. The idea was taken up

by a very large number of theorists, gradually refining and embellishing the properties of the W and adding the neutral component, Z. It is the stuff of brave scholars to give proper credit here. The theoretical work culminated in the electro-weak theory, elegantly described by Sidney Coleman (2) for the 1979 Nobel Award to Sheldon Glashow, Abdus Salam, and Steven Weinberg.

The experimental threads begin with the searches for W's carried out in the high energy neutrino experiments of 1964–65 at Brookhaven National Laboratory in New York and at CERN. The W would be produced in association with a charged muon when muon-type neutrinos impinged on a material target. Subsequently the W would decay into another charged muon and a neutrino. The trick was to observe two muons, one having a transverse momentum of half the W mass. At this time, the W mass was completely unknown, but the non-observation of the above reaction established a lower limit to the W mass of about two proton masses. Soon thereafter, two U.S. groups developed a technique for seeking W's in strong interaction collisions where the entire energy and intensity of the primary beam of 26 billion electron volts (GeV) (at Brookhaven) was used in the production process. Now the limit was raised to approximately five proton masses. This line of research was abandoned in the 1970's when the advances in weak interaction experiments gradually established the credibility of the unified electro-weak theory and its predictions of the masses